In-line characterization of polymer deformation in melt and solid phase processing*

P. D. Coates†, A. R. Haynes and R. G. Speight
Department of Mechanical and Manufacturing Engineering/IRC in Polymer Science and Technology, University of Bradford, Bradford, West Yorkshire, BD7 1DP, UK

Constitutive relationships obtained from in-process measurements on polymers that have been subjected to typical solid or melt phase processing strain–temperature–time histories can be used for enhanced modelling of deformation and flow (e.g. finite element analysis/computer aided design), or to provide new information on shear and extensional flows. In some circumstances in-line measurement may be the only practical route to reliable constitutive data. In the case of melts, such measurements may also be used for real time assessment of polymer state and for process control. The in-process measurements discussed in this paper are specifically concerned with 'in-line' rheometry, where pressure, temperature, stress, strain and strain rate measurements are made upon polymers in actual process geometries, under actual process conditions. Examples of accurate in-line measurements of polymer rheometry in an injection moulding nozzle and in a model solid phase forming process—uniaxial drawing of polymers—are discussed.

(Keywords: characterization; deformation; processing)

INTRODUCTION

Increasing sophistication of computer modelling and the drive for improved product quality provide two major stimuli for the area of research discussed in this paper[1]. Modelling of polymer melt or solid phase processing operations by finite element analysis or other numerical techniques requires a reliable numerical analysis technique (not discussed here) and accurate constitutive data. Results from computer numerical analysis of simple shear flows of polymer melts, for example, are most sensitive to changes in the viscosity–shear rate–temperature function, hence the importance of accurate constitutive data for input into the analysis. It is also important to use constitutive data which apply to the range of stress and strain rates being modelled. Modelling of solid phase deformation is similarly sensitive to the accuracy of the constitutive relationships employed[2]. Extensional flows and elasticity are increasingly recognized as important issues in polymer melt processing, yet these are not widely incorporated in commercial numerical analyses, largely because of the lack of reliable constitutive data.

The traditional approach to obtaining constitutive data for use in melt processing analysis and design is to use well-controlled laboratory rheometers[3,4]. However, the strain–strain rate–temperature–pressure history imposed on an element of polymer melt in such devices differs significantly from the history it would typically experience in melt processing.

The case of solid phase forming is a little different. Here, it is feasible to undertake uniaxial or biaxial 'off-line' tests which may be reasonable simulations of commercial processing. However, in many polymers, deformation is inhomogeneous (involving formation of local regions of high strain and strain rate gradients, i.e. necks), which has led to difficulties in obtaining reliable constitutive data for these materials using extensometry (strain gauge or optical), although earlier work by Coates and Ward[5,6] and recent studies by G'Sell *et al.*[7] address this problem.

The research reported in this paper is in the area of 'in-process' measurement. *Figure 1* shows schematically the potential of 'in-process' measurements for input into numerical analysis, or as raw data for real time process assessment and control, or for studies of molecular features on macroscopic flow behaviour. In-process measurements may be either 'in-line' or 'on-line'[1]. *On-line* measurement involves diverting a small stream of polymer to a rheometer connected to the processing equipment (clearly only feasible for melts), whereas *in-line* rheometers provide measurement on polymer in the actual process deformation or flow, i.e. under actual process stress, strain and temperature histories.

The research reported here focuses on two examples of rheological measurements, one concerning polymer melt processing and the other a model polymer solid phase processing operation, both obtained in-line with actual processes. At present, pressure or load, temperature and displacement (or dimension) provide the most useful in-process measurements. In the case of melts, several in-line rheometers have been designed and used in our laboratories since 1979, on injection moulding[8–13] (see also reports by other workers[14,15]) and extrusion

*Presented at 'Polymer Science and Technology—a conference to mark the 65th birthday of Professor Ian Ward FRS', 21–23 April 1993, University of Leeds, UK

†To whom correspondence should be addressed

0032-3861/94/18/3831–13

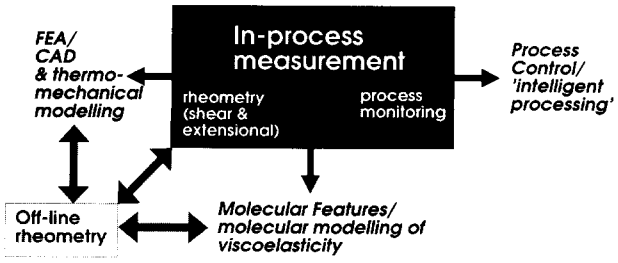

Figure 1 Schematic diagram showing the use of in-process measurements

processes[16,17], for characterization of the shear and extensional rheology of polymer melts and reacting systems, and for identifying control strategies. A novel on-line rheometer (Rosand Precision Ltd) is also currently being used in our research. The in-line rheometers employ accurate pressure and pressure drop measurements, and melt temperature assessment (including infra-red fast response sensors), for constant cross-section or converging flow geometries, allowing viscosity function determination for predominantly shear or extensional flows. Results from injection moulding and extrusion processing indicate the sensitivity of these measurements to certain molecular features and changes in the polymer during processing or variation in polymer feedstock, and provide comparisons with standard ('off-line') rheometry techniques, which do not subject the polymer to typical process histories.

In the case of solids—a far smaller fraction of the total polymer processing area—our non-contacting rheometry employs optical image analysis of specimens with printed orthogonal grids, which are subjected to uniaxial and biaxial tensile deformation in a computer monitored tensometer. The work reported here will deal only with uniaxial drawing. Although this is not a manufacturing process, our previous studies have shown that it does provide a good model of predominantly tensile processing operations[18]. Also, although gridding of the polymer is not practical for full production, it has been successfully used to enhance process knowledge in pilot runs and in manufacturing tests associated with our laboratories (e.g. in thermoforming). Thermal imaging of specimens is also used to monitor associated surface temperature profiles[17]. Sophisticated image capture hardware and software allows up to 16 frames to be captured at chosen times, providing for detailed measurement of the strain history of each element of the grid in the field of view. Together with synchronized draw load data, a process true axial (stress–strain–strain rate) curve can be constructed from a single specimen. Image capture rates are chosen to observe neck formation and propagation, to investigate flow rules, and to determine true axial (stress–strain–strain rate) surfaces. This research programme is run in collaboration with Ward *et al.* in the IRC group at Leeds University. Research is also proceeding into biaxial tension flow rules, in collaboration with the IRC group at Leeds[19]. Polyethylene, polypropylene (PP), unplasticized poly(vinyl chloride) (UPVC) and styrene butadiene rubber elastomers have recently been investigated in our laboratories, but only results from the polypropylene drawing studies will be presented here.

Studies on processing of polymer melts and polymer solids have traditionally been treated and reported separately; they are brought together here to emphasize that there are similarities in our studies, and to further the case for considering the behaviour of polymers across the (often diffuse) melt boundary. The studies of deformation of polymers in the solid and melt phases are being recognized as having increasingly common ground, for example with molecular network effects persisting into the melt phase. In the timescale of typical processing operations (mean residence times of minutes or less at the processing temperature), melts are not likely to lose all memory of their previous solid phase state. However, it is not in the scope of this paper to explore the depths of these similarities; here we describe experimental techniques (which clearly differ in practical outworking, but have a similar purpose) and particular results emerging from our studies to emphasize the value of in-line measurements. Details of the individual studies with fuller discussion will be published elsewhere.

EXPERIMENTAL

Injection moulding rheometry

The polymer melt studies reported here were undertaken on two fully instrumented, computer monitored injection moulding machines in our laboratories, a Sandretto 'Series Seven' 60 tonne hydraulic machine and a Cincinatti Milacron ACT30 30 tonne electric injection moulding machine. Both machines were fitted with instrumented nozzle rheometers, designed and built in-house. A view of the Sandretto machine installation is shown in *Figure 2*, showing two monitoring computers (one PC for rapid data capture for the primary injection phase, one for slower data capture largely associated with the plasticization phase). Data capture, using a Microlink interface and our own real-time C code software, is synchronized electronically using an output from the injection moulding machine parameter and sequence control computer (seen at the centre of *Figure 2* for the Sandretto machine). Data capture may be flexibly programmed at any rate, up to frequencies in excess of 1000 Hz, if required. Typically, process variables are monitored at 50 Hz.

A schematic diagram of the modular nozzle rheometer[10,11] fitted to the Sandretto machine is shown in *Figure 3*. This device is modular in that it allows a variety of sections to be mounted on the injection nozzle, each of which may contain a different transducer, and the tip may be either configured for conventional moulding or, as shown here, for in-line capillary rheometry. Normally, one or two fast response melt pressure transducers (Dynisco PT435A) are fitted. These have a combined error of $\pm 0.5\%$ full-scale deflection (f.s.d.), and a repeatability of better than $\pm 0.1\%$ f.s.d.; for accuracy, a fourth order polynomial calibration at the operating temperature has been employed. Relatively fast response thermocouples or, preferably, an infra-red temperature sensor (Dynisco MTT935A) are also mounted in the nozzle.

Two pressure transducers are employed in 'air shots', in which polymer is injected into air rather than into a closed mould. Two pressure transducers are employed in this case in order to obtain a comparison with results from our 'off-line' Rosand Precision Ltd RH7 twin bore capillary rheometer: an estimate of pressure is required at a point in the nozzle equivalent to the location of the centre line of the single pressure transducer in the RH7, namely 10 mm from the capillary entrance. It is not possible to site a pressure sensor at this point in the nozzle, because of nozzle mounting requirements. Clearly,

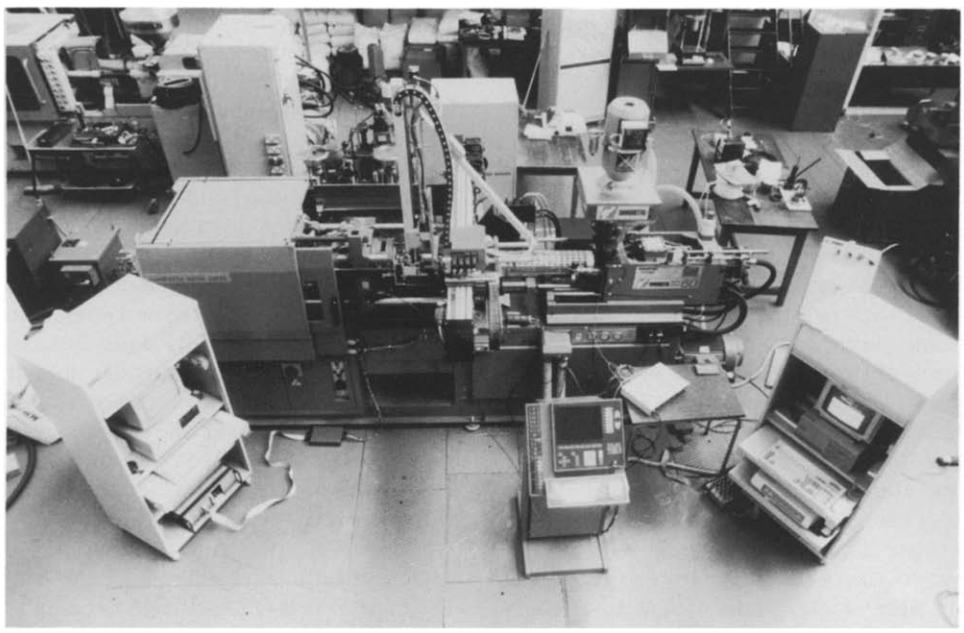

Figure 2 A view of the computer monitored Sandretto Serie Seven injection moulding facility in our laboratories

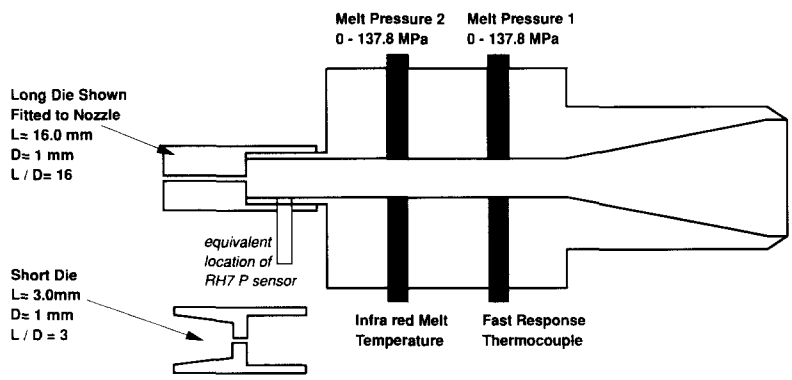

Figure 3 Schematic diagram of the modular nozzle rheometer used with the Sandretto injection moulding machine

three pressure sensors in line would be better for even more accurate extrapolation, but the use of two provides a practical compromise; also, there is only a small pressure difference between the sensors (typically only a few bar). It is also our experience that both transducers and the extrapolated pressure value follow the same variations experimentally[19]. When undertaking actual injection moulding, the nozzle has normally been re-configured to replace the capillary die shown in *Figure 3* with a suitable nozzle exit, and to employ a single pressure sensor and a temperature sensor (normally infra-red) by removing the nozzle module containing pressure sensor 2 (see *Figure 3*). This avoids having too large a melt reservoir at the nozzle, yet still allows valuable in-line process data to be obtained.

The nozzle rheometer fitted to the CM ACT30 is similar in design but smaller (in keeping with the lower volumetric capacity of this machine). Currently only one pressure and one temperature sensor is fitted. Both machines are further extensively instrumented, in particular for screw displacement and screw injection velocity and mould conditions, in addition to the standard commercial instrumentation for machine functions.

The nozzle tips for both machines may also be configured to simulate the geometry of our RH7 capillary rheometer, and allow fitting of dies with a range of entry angles. Two sets of 1 mm diameter capillary dies with semi-angles from 30° to 90° (flat entry) are available, in length to diameter ratios (L/D) of 16/1 and approximately zero (i.e. 'zero length' dies—in practice a land length of 0.25 mm is used, giving $L/D = 0.25/1$), plus a flat entry die with $L/D = 3/1$.

Polymers used in the injection rheometry studies reported here were polyoxymethylene homopolymers from the DuPont Delrin II series, grades 100, 500 and 900F in order of decreasing molecular weights (melt flow rates at 190°C, 2.16 kg load are 1–3, 12–16 and 19–33 g/10 min, respectively) injected at set barrel and nozzle temperatures of 215°C, at various injection velocities. Some results are also presented for a high density polyethylene (HDPE; BP Chemicals' HD5050EA, a copolymer with a narrow molecular weight distribution, melt flow rate 26 g/10 min at 190°C, 2.16 kg load) at a set nozzle temperature of 190°C.

Solid phase rheometry

The uniaxial tensile deformation of polymers is being studied using an Instron 1026 tensile tester at Bradford, and a unique biaxial tester in our Leeds IRC laboratories. The work reported here refers only to the Instron, which

also has a purpose-built oven with precision temperature control, a window for optical or thermal imaging, and variable surface heat transfer capability. The image capture equipment comprises a Pulnix CCD camera with a selection of lenses, and frame capture hardware (Data Translation Inc.) housed in a PC. The system allows up to 16 512 × 512 pixel frames to be captured at controlled time intervals down to 40 ms between frames, each frame being stored to hard disk. Uniaxial tensile drawing load is monitored simultaneously by the computer, using direct memory access, with precision synchronization of load signal and frame capture. Image analysis typically involves identification of the displacements of silk-screen printed orthogonal grids ($\frac{1}{16}$ inch = 1.59 mm pitch in the present case) on polymer dumbbell specimens, by following light intensity peaks and troughs; analysis is undertaken either on the frame capture computer or on a separate IBM system using the powerful Image Assistant image analysis software library.

Results for PP copolymers (ICI GSE16) are reported here; all specimens were single dumbbells, with 25 mm gauge length, 10 mm gauge width and 4.5 mm thickness, with a dumbbell shoulder radius of 5 mm; these were drawn at 110 ± 1°C (an optimum drawing temperature for property enhancement in these materials[18]), at crosshead rates between 5 and 500 mm min^{-1}.

Image analysis of the positions of the orthogonal grid lines on the polymer dumbbell specimens in a frame captured at time t provides a measure of local axial strain for each originally orthogonal element, which corresponds to the axial stress calculated from the monitored load at time t.

If the original element has width w, axial length z and thickness h at time zero, and after time t has axial length z_1, then the axial tensile strain at time t is

$$\varepsilon_{zz} = \ln \lambda = \ln(z_1/z)$$

where λ = draw ratio. Assuming deformation at constant volume, the elemental cross-sectional area on which the axial load at time t, $L(t)$, acts, is

$$A = wh/\lambda$$

hence the axial stress acting on the element at time t is

$$\sigma_{zz} = L_{el}/A$$

where L_{el} is the portion of the load $L(t)$ acting axially on the element (the load is assumed to be shared equally by all elements across the gauge width in the gauge length region). If deformation did not occur at constant volume, a Poisson's ratio effect, as a function of draw ratio if necessary, could be included in the stress calculation.

Examination of a time series of frames allows calculation of the associated local strain rate in the element: the axial strain rate assessed for deformation in moving from frame i to frame $i+1$ is

$$\dot{\varepsilon} = \frac{\varepsilon_{i+1} - \varepsilon_i}{t_{i+1} - t_i}$$

A typical experiment involves capture of 16 frames at chosen times, followed by analysis of axial strains, strain rates and stresses for around 12 elements along a chosen line; in the work reported here, the specimen axial centre line is used. By these means, a process true axial (stress–strain–strain rate) curve is obtained from a single tensile specimen. Altering the extension rate provides similar data but in a different axial strain rate region. It is assumed that the polymer deforms at constant volume, and that the draw load is shared equally by each element across (i.e. transverse to the draw direction) the gauge length of the specimen.

The image analysis technique provides a rapid, non-contacting method of obtaining extensive solid phase deformation data from a limited number of tests, and benefits from the advantages discussed by G'Sell *et al.*[7]. It also provides a means of obtaining neck profiles for different polymers using edge detection algorithms. The work reported here is complementary to that of G'Sell *et al.*[7] in that they deal with cylindrical specimens of 6 mm diameter and zero gauge length, and a shoulder radius of 20 mm. They monitor (by image capture) the centre line diameter of the specimen and programme the tensile tester to achieve constant axial extensional strain rate at this centre line, although the strain rates achieved in their experiments are limited to relatively low values ($\sim 10^{-2}$ s^{-1}) to remain in the approximately isothermal region, a limit partly imposed by the practical need for their specimens to be at least 6 mm diameter. In our case, similar specimens, or thick rectangular cross-section specimens (as reported here), or thin films may be studied using grid displacement measurement or edge detection. However, the facility for freely programmed extension is only currently available on our biaxial stretching equipment. The work of G'Sell *et al.* provides true stress–strain–strain rate data under carefully controlled deformation conditions, primarily for material property measurement. The work pursued in our laboratories is broader in context, in that any geometry specimen may be studied to generate actual process stress–strain–strain rate data; our equipment could also be transported to manufacturing or testing sites for data capture (including synchronous load capture, with appropriate interfacing).

RESULTS

Injection moulding in-line rheometry

Figure 4 shows a typical melt injection pressure–time plot for Delrin II 500 at 215°C set nozzle temperature, with screw displacement superimposed, for an 'air-shot' on the Sandretto machine. The nozzle rheometer was used with the long die, two melt pressure transducers (see Experimental section) and two thermocouples but no injection mould, simulating a capillary rheometer operation. The injection velocities for air shots are low compared with actual injection moulding, because even low injection rates produce high values of wall shear rate in the nozzle capillary. The nozzle can also be configured for standard injection moulding into a cavity, as indicated in the Experimental section, now employing one pressure sensor. *Figure 5* shows average injection pressure from 10 cycles *versus* time for the same polymer on the Sandretto machine, but with the nozzle now configured to inject into a family container tool, and a typical injection velocity, here 30 mm s^{-1}. Standard deviation of nozzle mean melt pressure is superimposed in *Figure 5*. This figure highlights important features of in-line nozzle rheometry, which have been found to be applicable to both air shots and actual mouldings; regions of higher standard deviation in the primary injection phase (0–1.7 s in *Figure 5*) are associated with process 'noise' introduced by screw accelerations and decelerations, for example. It is therefore desirable to collect data on the rheology of melts in the region of lowest standard deviation of

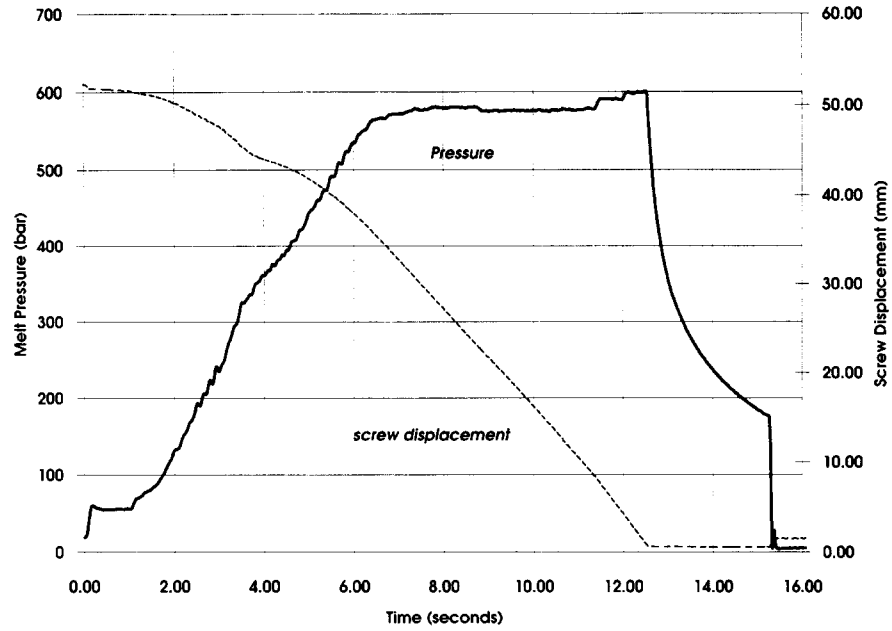

Figure 4 In-line nozzle rheometer, 'air shot': melt pressure at capillary die entrance and injection screw displacement *versus* time, for injection through the long capillary ($L/D = 16/1$), for polyoxymethylene homopolymer (Delrin II 500) at $5\,mm\,s^{-1}$ injection speed (volumetric flow rate $6.2 \times 10^{-6}\,m^3\,s^{-1}$), 215°C set nozzle temperature

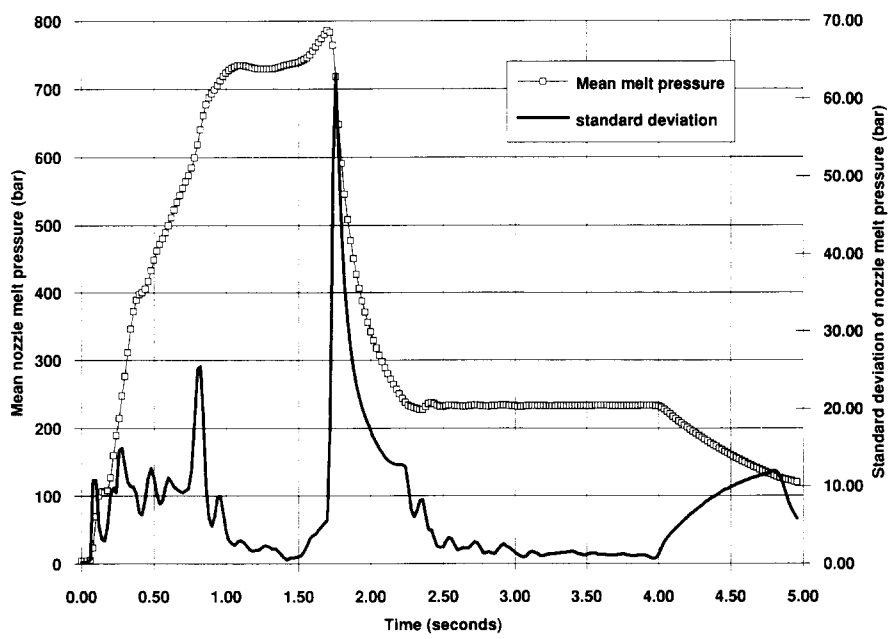

Figure 5 In-line nozzle rheometer, moulding: average melt injection pressure from 10 cycles for injection moulding of Delrin II 500 in family container tool, at 215°C set nozzle temperature

injection pressure (1.40–1.50 s in *Figure 5*) because changes in the measured pressures (or pressure drops) in this region of minimum standard deviation will best reflect changes in the polymer melt rheology. Our experimental studies[13], in both the laboratory and industry (on various injection moulding machines and with various tools), indicate that the injection moulding tool used will influence the actual shape of the mean melt pressure–time curve, and different machines will exhibit different dynamics and noise levels; however, low standard deviation regions have always been identified, as in *Figure 5*.

Infra-red temperature measurements have been found[13] to follow the rise in pressure, reflecting the shear heating of the polymer as it undergoes high shear rate flows. Typically a temperature rise of around 8°C is detected for injections such as those represented in *Figure 5*, in agreement with bulk temperature measurement of polymer melt collected immediately on exiting the capillary in nozzle rheometer air shots (the bulk temperature rises approximately linearly with injection velocity). Melt temperature in the nozzle has been found to be influenced by melt pressure in the nozzle for periods of screw acceleration, and by polymer melt compression during primary injection, effects which will be reported elsewhere.

Injection through the in-line nozzle rheometer at various injection velocities allows a typical apparent wall shear stress–apparent wall shear rate curve to be constructed. Using standard capillary rheometry analysis

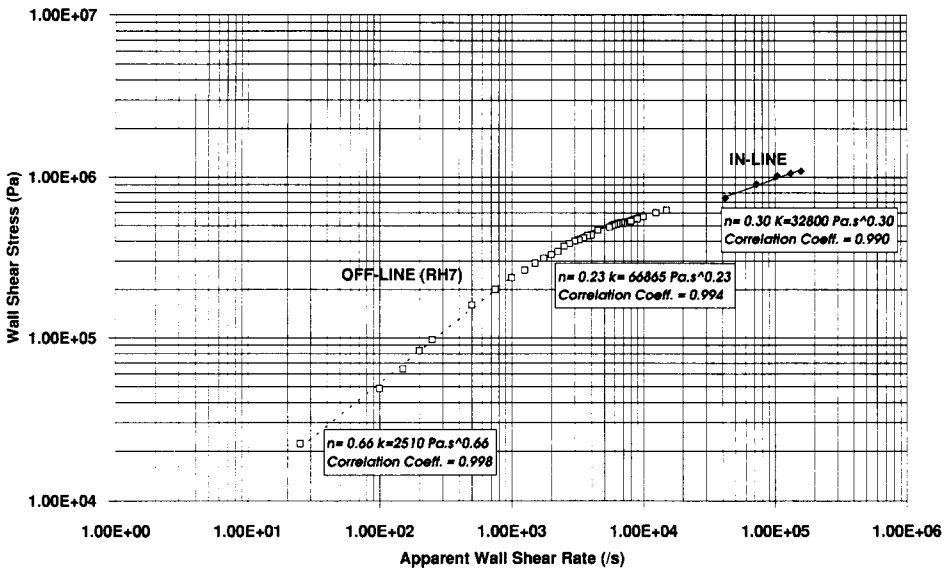

Figure 6 Off-line (Rosand RH7) and in-line capillary rheometry: uncorrected shear stress–shear rate plot for Delrin II 500 at 215°C set temperature

Table 1 Off-line and in-line power law fits for Delrin II 500 ($\tau = K\dot{\gamma}_{app}^{n}$)

	Wall shear rate range (s^{-1})	n	K (Pa s^n)	Correlation coefficient of power law fit
Off line	25–10^3	0.66	2510	0.998
	6×10^3–1.5×10^4	0.23	66900	0.994
In-line	4.2×10^4–1.6×10^5	0.30	32800	0.990

for steady state laminar flows, the capillary wall shear stress is

$$\tau = \frac{r\Delta P}{2L}$$

where r = capillary radius, L = capillary length and ΔP = pressure drop in capillary; and apparent shear rate at the capillary wall, for volumetric flow rate Q $m^3 s^{-1}$, is

$$\dot{\gamma}_{app} = \frac{4Q}{\pi r^3}$$

Figure 6 shows an uncorrected shear stress–shear rate plot for Delrin II 500 (data not Bagley or Rabinowitsch corrected in both cases, matching geometries were used), and contains data collected by standard off-line capillary rheometry using a Rosand RH7 twin bore capillary rheometer at 215°C set barrel temperature, and the in-line nozzle rheometer fitted to the Sandretto machine, also at a set nozzle temperature of 215°C. Conventional power law fits have been made to the data for regions of low, medium and high wall shear rate, giving the values of viscosity coefficient, K, and power law index, n, shown in *Table 1*. The lack of overlap of data between the two tests is due mainly to the problem in obtaining relatively low shear rate data in-line for the capillary geometries chosen (these were chosen in the first instance to be similar to those of the RH7), since 'low' in-line wall shear rates (e.g. of the order of $10^4 s^{-1}$ or less) would require extremely low injection velocities, which are not well controlled on injection moulding machines. Larger diameter capillaries provide a partial solution to this problem, but were not available for these experiments.

It is clear from *Figure 6* that, as expected, a single power law expression cannot be used to describe the rheology of the polyoxymethylene for the range of wall shear rates investigated. (From an engineering viewpoint, it is clearly feasible to curve fit using higher order polynomials.) It is also apparent that the higher wall shear rate results from off-line capillary rheometry appear to be in reasonable agreement with those from in-line nozzle rheometry, although care is required in interpretation, for example if any leakage flows occur during process measurements. The correlation coefficient, measuring the goodness of fit of the power law, is high in all cases, despite a general finding of our work that in-process measurements tend to reflect process and machinery related variations, and may consequently exhibit greater standard deviations than off-line measurements, for polymers that do not change state significantly during testing.

The relatively good agreement observed for off-line and in-line rheometry of Delrin II 500 is further reflected in *Figure 7* and *Table 2*, where results for the higher and lower molecular weight polyoxymethylenes are shown.

Figure 8 shows viscosity data derived from the uncorrected shear stress and wall shear rate measurements, reflecting the expected lower viscosities for lower molecular weight polyoxymethylenes, and the relatively good agreement between off-line and in-line data at high wall shear rates for these materials. The rapid fall in viscosity with wall shear rate is due partly to the non-Newtonian behaviour of the melts and partly to viscous shear heating, as noted earlier (these are non-isothermal flows, hence accurate temperature determination is vital in both off-line and in-line rheometry). In general, results should be normalized to a chosen temperature, but there are insufficient in-line results here for accurate normalization. However, other tests at a range of nozzle temperatures indicate that the major influence on the fall in shear stress at higher shear rates is not due to viscous heating, since viscous heating accounts for a fall in shear stress with temperature of approximately 1 kPa $°C^{-1}$. The fall in viscosity with shear rate or shear stress is therefore mainly attributed to shear thinning. Similar trends in shear stress with shear rate

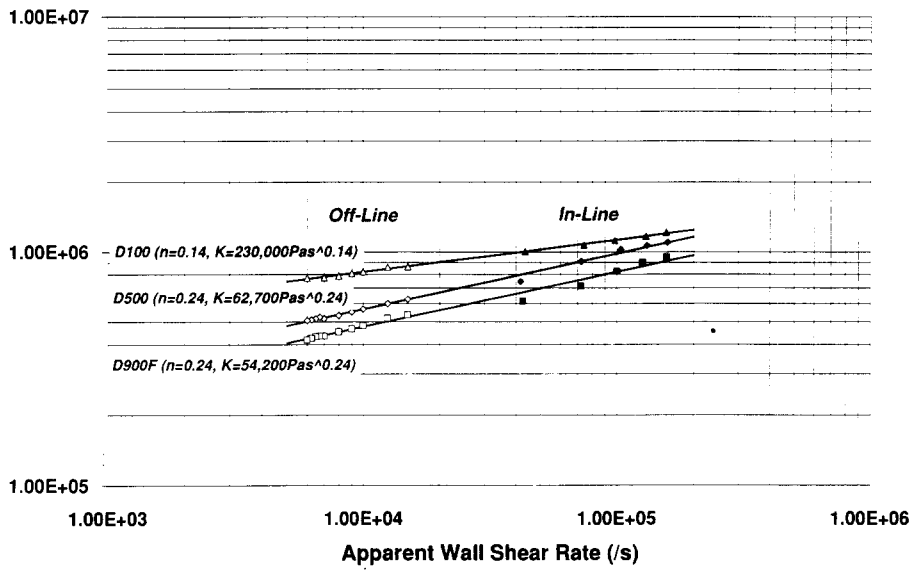

Figure 7 Off-line and in-line rheometry: comparison for the high shear rate region for Delrin II 500 at 215°C set temperature

Table 2 Combined off-line and in-line power law fits at medium to high shear rates: Delrin II, wall shear rate range 6×10^3–$1.6 \times 10^5\ s^{-1}$

	n	K (Pa s^n)	Correlation coefficient of power law fit
Delrin II 100	0.14	230 000	0.999
Delrin II 500	0.24	62 700	0.997
Delrin II 900F	0.24	54 200	0.993

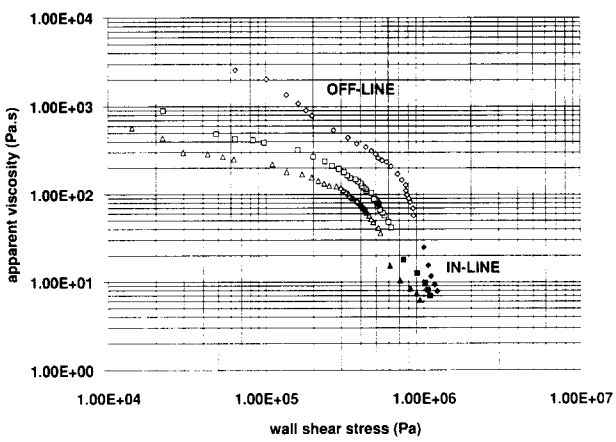

Figure 8 Off-line and in-line rheometry: apparent viscosity *versus* uncorrected wall shear stress for three molecular weight grades of polyoxymethylene homopolymer, Delrin II 100 (◇, ◆), 500 (□, ■) and 900F (△, ▲) at 215°C set temperature

and viscosity with shear stress were observed for the HDPE studied.

Figure 9 shows results from Chohan *et al.*[20] from entry pressure measurements for HDPE HD5050EA at the in-line nozzle capillaries (CM ACT30 injection moulding machine) and off-line (Rosand RH7) capillaries. 'Zero length' dies of varying entrance semi-angles were used: the land length in these dies is 0.25 mm, i.e. $L/D = 0.25/1$. Entry pressure measurements have traditionally been used as an indicator of extensional viscosity[3]. The purpose here is not to consider the effect of entry angle in detail (such as the minimum in entry pressure observed at mid-range semi-angles) but to indicate the significant result that off-line and in-line measurements differ by greater amounts in predominantly extensional flows than in shear flows. It therefore appears to be important to consider carefully whether in-line measurements should be used as input to melt flow modelling where significant extensional flows are expected (e.g. at strongly convergent geometries such as gates).

Considering briefly the use of in-line measurements for eventual process control (a move towards 'intelligent processing'[1]), *Figure 10* shows the use of in-line pressure measurements for process assessment, here for the Sandretto machine tests for moulding using the family container tool. Taking the region of low standard deviation of injection pressure shown in *Figure 5* for these mouldings, a pressure integral for a specific period within the velocity controlled primary injection phase (here 1.40–1.50 s) has been found to provide a sensitive indicator of changes in the polymer being processed. Different bags of polymer from the same lot number were processed, and the pressure integral results shown in *Figure 10* clearly demonstrate that it has been possible to distinguish between the different bags. This ability to distinguish changes in the polymer has been found to be sensitive—the differences are greater than the statistical variations in the parameters being monitored—and has clear implications for assessment of process stability, or for detecting changes in the process which could form the basis of a control strategy. Similar results have been observed for HDPE and acrylonitrile-butadiene–styrene.

Finally, in this subsection, a particularly significant result from the viewpoint of exploitation of in-line measurements for process control is presented. Pressure integrals obtained from in-line measurements, using regions of low standard deviation in melt pressure in both the primary injection (see *Figure 5*) and packing phases, have been shown to correlate with off-line assessments of injection moulding product quality such as product weight or a chosen dimension. *Figure 11* shows such results for an HDPE container moulding (*Figure 5* shows typical mean injection data for this mould), now using a packing phase melt pressure integral for a specific period in the packing phase, which has been found to

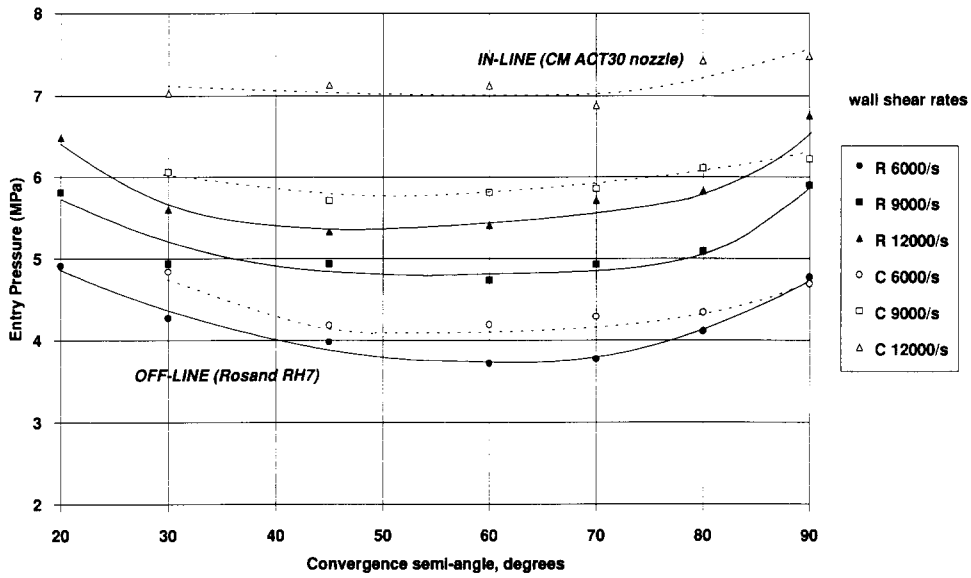

Figure 9 Off-line (Rosand RH7) and in-line rheometry: entry pressure *versus* die entry convergence semi-angle for HDPE at 190°C (R = Rosand RH7, C = injection nozzle rheometer on CM ACT30)

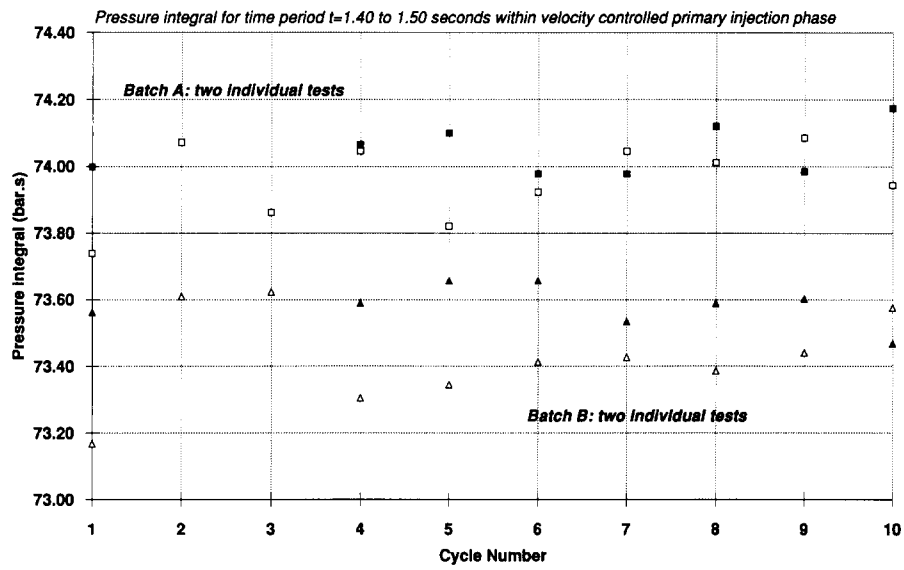

Figure 10 Use of in-line melt pressure profile integral from a selected low standard deviation region within the velocity controlled primary injection phase, for assessment of polymer batch-to-batch variation and experiment repeatability inside one batch

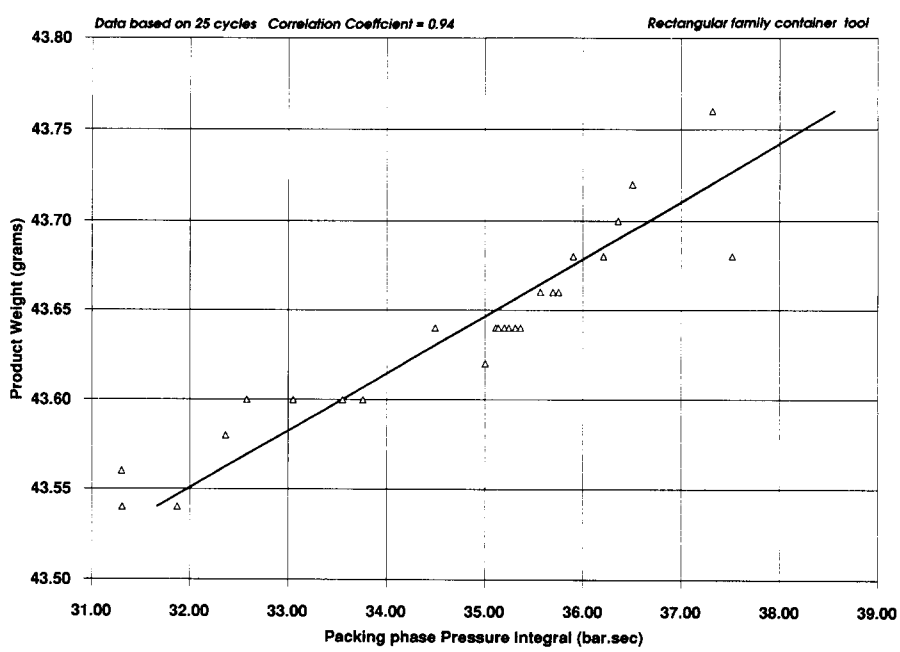

Figure 11 Typical correlation of pressure profile integral for low standard deviation region within the packing phase with product weight for HDPE injection moulding, 25 cycles at 190°C set nozzle temperature; correlation coefficient = 0.94

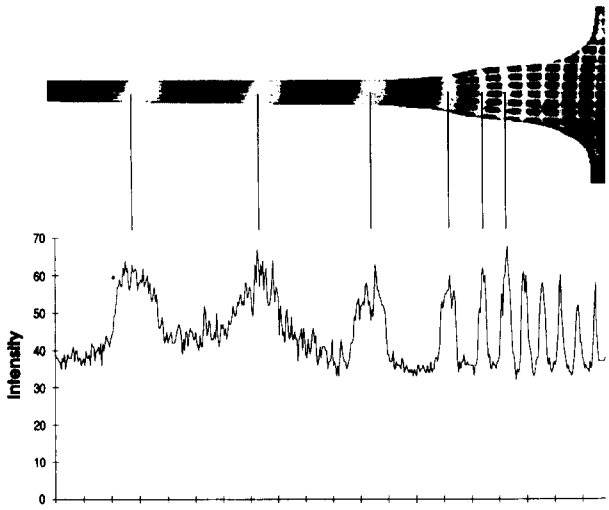

Figure 12 Line profile of light intensity for the axial centre line of GSE16 PP copolymer dumbbell undergoing uniaxial drawing at 110°C

correlate with product weight, which here represents the weight of the pin-gated cavities, not including the sprue or short runners. These results are typical of those observed for other polymers used in our studies.

Hydraulic injection pressure and cavity pressure measurements have also been studied[13] but are not presented here. These may prove useful in specific cases: certainly, the use of low cost hydraulic injection pressure measurements, given suitably low levels of signal noise, would be particularly attractive for process control, whereas cavity pressure measurements are often prohibitively expensive. A full comparison will be published elsewhere.

Solid phase drawing in-line rheometry

Figure 12 shows a line profile of intensity, the raw data for our image analysis studies. Identification of the intensity peaks can be achieved with high accuracy, allowing monitoring of the lengths of elements marked by the transverse gridlines. Drawing of a single specimen

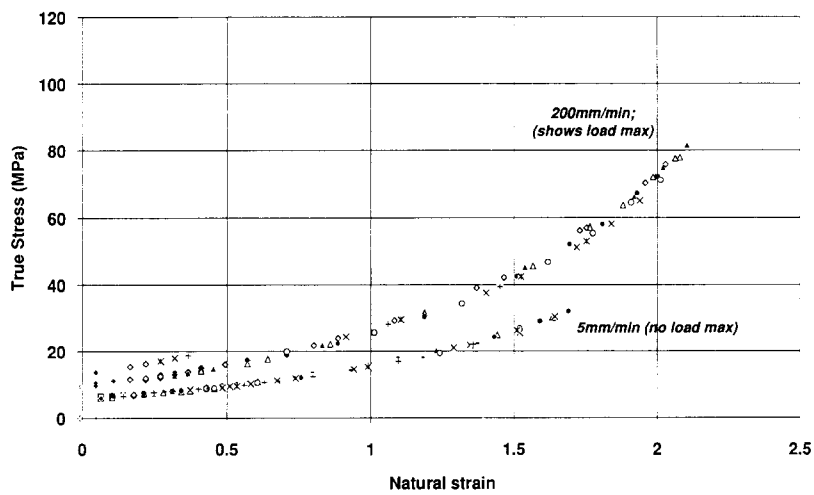

Figure 13 Image analysis: process true (stress–strain) curves for GSE16 PP copolymer at 110°C, at extension rates of 200 mm min^{-1} (for which a load maximum is observed) and 5 mm min^{-1} (no load maximum); these curves are made up of stress–strain values for individual grid elements, each element having a specific symbol; frames captured at 3 s and 100 s intervals, respectively

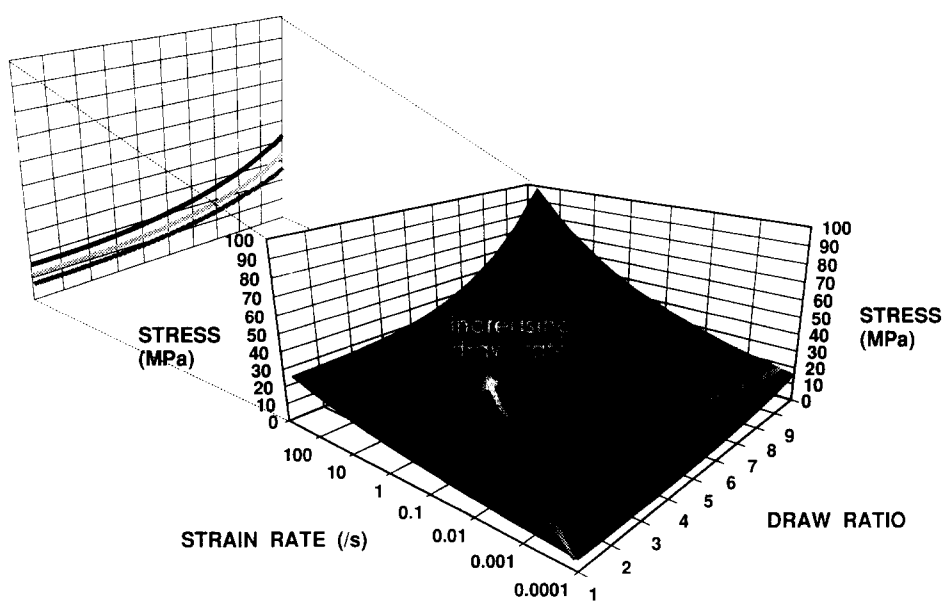

Figure 14 Schematic process true stress–draw ratio curves on a true stress–draw ratio–true strain rate–constant temperature surface, and projection showing process stress–strain curves (shown as isothermal)

at a fixed crosshead speed then allows a process axial stress–strain curve to be constructed by plotting the axial stress–axial strain points for each element along the centre line of the specimen. Two typical examples are shown in *Figure 13* for a PP copolymer drawn at 110°C. The 200 mm min^{-1} case involved frame capture every 3 s, whereas the 5 mm min^{-1} case used frame capture every 100 s. It should be noted that the curves in *Figure 13* are not constant extensional strain rate curves; they involve elements undergoing a maximum in extensional strain rate as they pass through the neck[5,6]. The 200 mm min^{-1} curve also shows a particular feature of interest, namely stress values that lie above the main curve at strains up to 0.4. These higher values simply reflect the existence of a load maximum during the drawing process, and the fact that they appear to fall on a single higher curve is an artefact of the frame capture time—one frame was captured at a particular time in the load peak. If the frame capture had been more rapid (as in the experiment depicted in *Figure 18*), more frames would be captured in the period of the load peak, leading to several levels of stress curves above the main curve, each level corresponding to a single frame. Drawing the PP at 5 mm min^{-1} at 110°C (*Figure 13*) incurs no load maximum, so no higher stress values are detected.

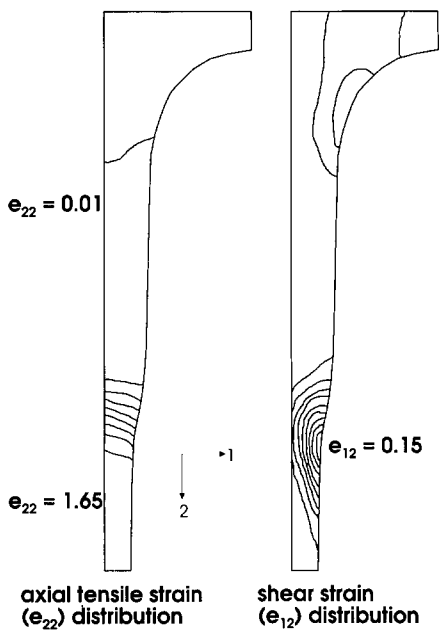

Figure 15 Axial extension strain (e_{22}) and shear strain (e_{12}) distributions predicted by ABAQUS two-dimensional finite element analysis, using constitutive data obtained from image analysis for GSE16 PP, showing the neck region (results for 9 mm loading displacement of transverse centre line of a dumbbell specimen of equivalent geometry to those used experimentally)

The relevance of such curves to solid phase drawing processes is shown schematically in *Figure 14*. Here, the existence of a true axial (stress–strain–strain rate) surface for uniaxial deformation at a constant temperature is employed: a process stress–strain curve, such as shown in *Figure 13*, represents a path across this surface. The nature of this surface, and its application to deformation processes such as hydrostatic extrusion and die drawing, has been discussed previously[5,6]. In-line measurement by image analysis now provides an efficient way of generating data which will allow such surfaces to be constructed. *Figure 14*, however, indicates that single tensile tests of the kind employed in the work reported here will be insufficient—redrawing of highly strained polymer will be required to obtain data at a wider range of strain rates at high strains. Alternatively, constant strain rate tests at higher strain rates are required, and these are areas of our continuing research.

The process axial stress–strain curves shown in *Figure 13* may also be used as input to finite element models of deformation processes. *Figure 15* shows typical output from an ABAQUS finite element model, using image analysis generated constitutive data for PP GSE16 as input. The finite element analysis studies are exploring a combined (not coupled) stepwise mechanics and thermal analysis (the latter is not yet fully implemented), applying incremental displacement loading to the centre line of a single dumbbell specimen. It has been possible to show necking, and the predicted distribution of extensional strain along the specimen centre line in the draw direction agrees well with that observed by image analysis, as shown in *Figure 16*. This is an encouraging result, because it shows that the finite element analysis is not distorting

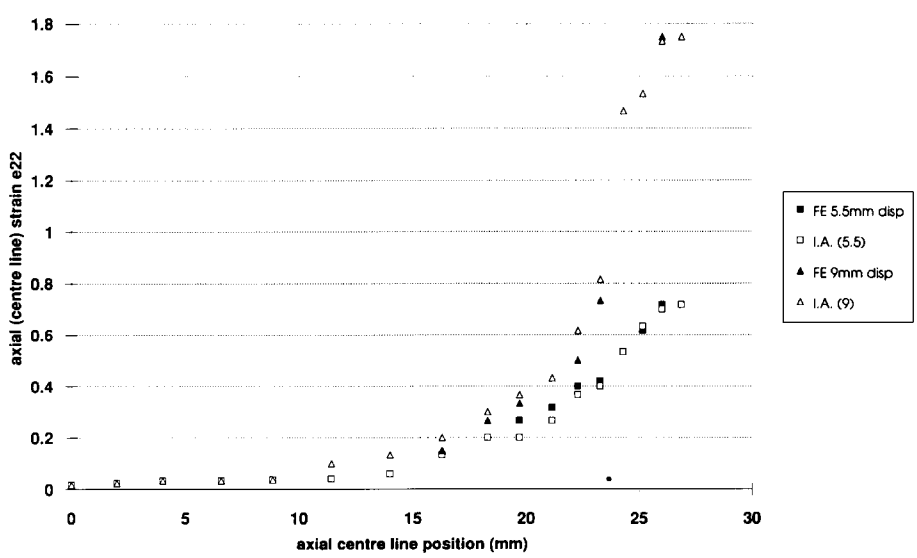

Figure 16 Image analysis results compared with finite element predictions for GSE16 PP (finite element using constitutive data obtained from image analysis), showing agreement of predicted axial strain with experimental image analysis measurements

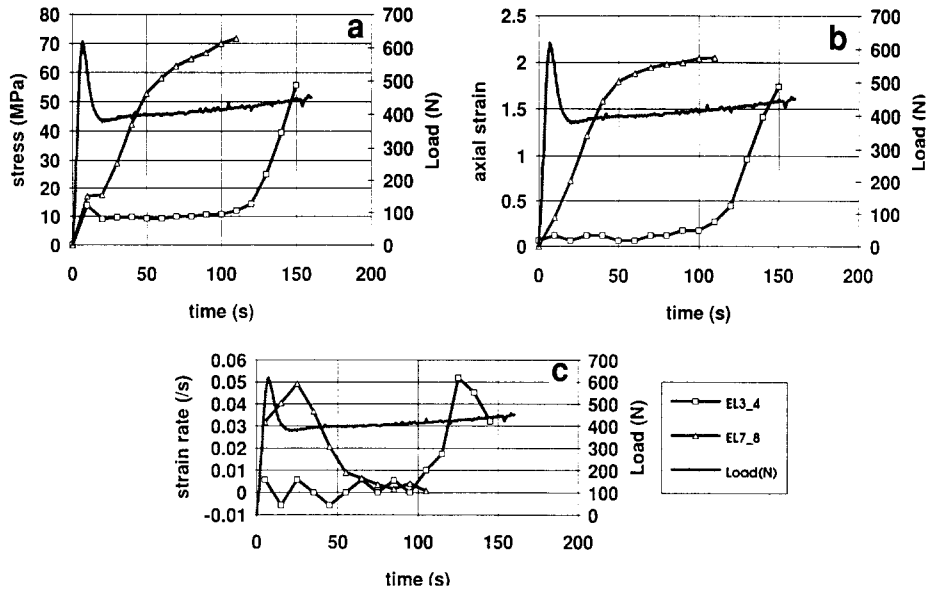

Figure 17 (a) True stress, (b) strain and (c) strain rate *versus* time for two grid elements, with draw load superimposed, for GSE16 PP dumbbell drawn at 110°C at 50 mm min^{-1}: el3_4 is distant from the neck initiation; el7_8 is close to the neck initiation region at the start of the test; both are axial centre line elements

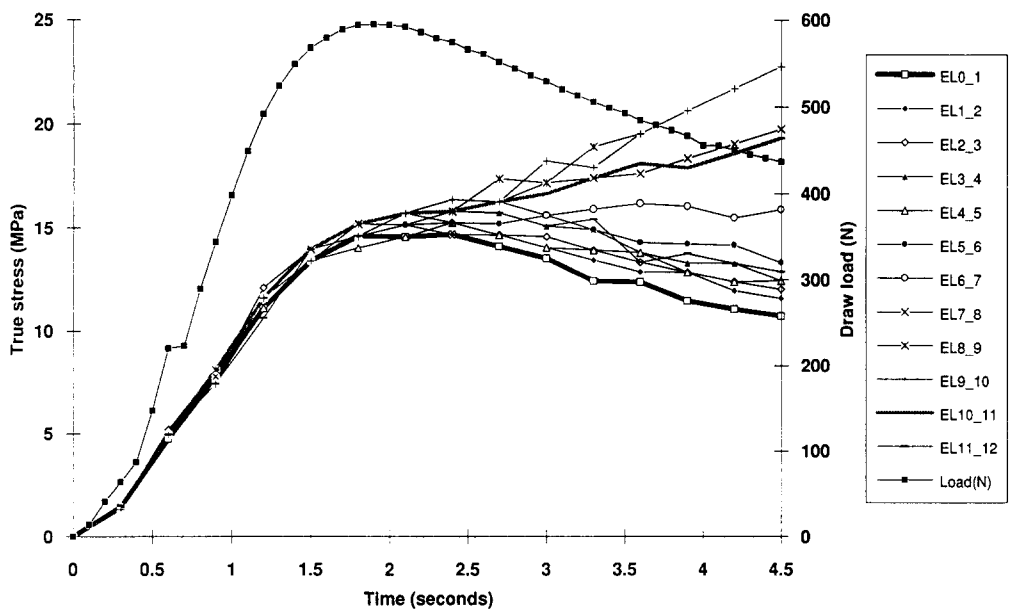

Figure 18 Image analysis: true axial stress *versus* time for axial centre line elements for GSE16 PP drawn at 200 mm min^{-1} at 110°C, frames captured at 0.3 s intervals: el0_1 is distant from neck initiation region; el10_11 is close to the neck initiation region at the start of the test

the input data, and hence might be used to predict deformations for which we do not have, or cannot easily obtain, experimental data.

Finally, the in-line deformation measurements have been used to observe aspects of neck initiation and propagation. *Figure 17* shows stress, strain and strain rate measurements for PP drawn at 50 mm min^{-1} at 110°C, for two elements: el3_4 was near the dumbbell shoulder and hence somewhat distant from neck initiation (which occurred near to the centre of the gauge length), whereas el7_8 was located close to the region of neck initiation. The load–time curve for drawing is superimposed on each part of *Figure 17*. It is clear that the load maximum influences elemental axial stress, and that both elements see a strain rate peak as they pass through the neck (or the neck passes through them); the similarity of the strain rate peaks suggests that the neck profile does not change significantly during the test. This observation is in keeping with many other experiments that we have undertaken, i.e. the neck profile, once established, remains approximately constant. Neck initiation appears to involve a higher strain rate peak; the detail of these results will be presented elsewhere. Operating at a much greater frame capture rate allows us to observe more closely a particular strain region: *Figure 18* shows data from drawing of PP at 200 mm min^{-1} at 110°C, with a frame capture interval of 0.3 s. The total monitoring time of 4.5 s covers the major part of the observed load maximum. *Figure 18* indicates the calculated axial stresses in each axial element (stress calculated from the load and elemental axial strain), and it is clear that the axial stress appears to fall in elements distant from the neck initiation, e.g. el0_1, and to rise consistently in elements near to the region of neck initiation, e.g. el10_11.

Our image analysis studies have included a range of polyolefins, UPVC and elastomers, which are outside the scope of this paper. They include studies of the effect of morphology on drawing behaviour for specific polyolefins, and are being extended to molecular weight differences.

DISCUSSION

The research presented in this paper has covered solid and melt phase processing, and we have attempted to show that in-process measurements may be used to obtain sensitive assessment of polymer rheology, which may then be exploited in the modelling of processing. In the case of melts, good agreement was noted between off-line and in-line tests for the reasonably 'well-behaved' polymers studied (i.e. those that do not change significantly during the process timescale under process conditions). A power law constitutive model (or higher order polynomial curve fit) is often used in finite element modelling, but the danger is that lower shear rate data are used to model higher shear rate flows, because of lack of reliable experimental data. Low shear rate data, such as those collected by off-line capillary rheometry, are acceptable for modelling injection moulding cavity shear flows (and extrusion die shear flows in general), but not for regions of high shear rates, such as injection nozzles, gates and narrow runners.

Good agreement between off-line and in-line shear data is, however, not likely to occur when changes in the polymer state occur during processing, e.g. by reaction, thermal degradation or chain scission. Here, in-line rheometry will provide an essential tool, and may be the only route to obtaining reliable data. The chemorheology of a range of polymers is the subject of a wider programme of research on reactive processing of polymers in our laboratories; degradation, scission and possibly unwanted reaction effects form part of our broader in-line rheometry studies. Also, greater differences between off-line and in-line rheometry have been observed in the case of extensional flows; this will have to be considered by modellers in building or obtaining extensional constitutive relationships, as the techniques for handling extensional flows increase.

In-line rheometry of melts proves to be sensitive to gross changes in the polymer, such as molecular weight grade, and also to statistical variations (which may relate to variations in molecular weight distribution) in different supplies of the same polymer grade.

The use of in-line rheometry for process assessment has been demonstrated: this is now being researched in collaboration with industrial partners. Initial results confirm our laboratory findings and point to a sensitive yet robust technique for assessing process trends and product quality. This is forming the basis of a closed loop control strategy which embraces and builds upon statistical process control, and is building towards intelligent processing of polymers, namely assessment of the polymer state being used to maintain automatically the process inside a chosen range of product quality.

In-line rheometry is also finding increasing application (and is currently being further developed) in solid phase forming of polymers. The in-line image analysis technique has proven to be a powerful, flexible method of obtaining new data concerning neck initiation and propagation, which will provide new insights into polymer deformation. The ability to capture strain data synchronized with draw load data at precisely timed intervals opens up new opportunities for studying the true stress–strain–strain rate behaviour of polymers, for both homogeneous and inhomogeneous deformation. This should provide a useful way of testing and developing models of deformation, investigating the existence of true (stress–strain–strain rate) surfaces for uniaxial deformation, and investigating whether these concepts apply to biaxial deformation. Unlike the case of in-line rheometry for melts, the solid phase rheometry has focused entirely on extensional behaviour (since this is so dominant in uniaxial deformation); shear behaviour is not ignored, but appears in the finite element studies (e.g. *Figure 15*).

In addition, the image analysis data have been used successfully as input to finite element models, providing accurate deformation data. This has allowed us to test reliably the finite element methodology employed, and gives confidence to apply the technique to problems that would be difficult or expensive to investigate experimentally. We have begun to model through-thickness effects, and our experimental work is being extended to obtain three-dimensional images, using two CCD cameras. The technique is also being adapted for use outside the laboratory: our recent developments allow precision synchronization signals (which are vital for correct data interpretation) to be recorded, together with the optical data, on commercial VHS video as the input for our image analysis system.

In common with in-line rheometry for melts, the data generated for solid phase forming are sensitive to differences in the polymer under test: molecular weight and morphology differences are readily observable. Fuller results will be reported elsewhere.

CONCLUDING COMMENTS

Results from melt processing, here injection moulding nozzle rheometry, and solid phase drawing of polymers have been used to demonstrate the sensitivity and usefulness of in-line rheometry for improved understanding of the processing operations, and for obtaining constitutive data from polymers that have been subjected to actual process histories. In-process measurement is proving to be a powerful technique for such rheological measurements, for use in process modelling and process control.

ACKNOWLEDGEMENTS

The authors are grateful for the support of SERC and a range of industrial collaborators, including Birkbys Plastics Ltd, BP Chemicals, DuPont UK, Dynisco, ICI, Ford Motor Co., IBM UK Laboratories and Sandretto UK, for the research reported here, and to Dr A. Mimaroglu for finite element studies.

REFERENCES

1 Coates, P. D. Plenary paper, Proceedings of 3rd International Conference on Polymer Processing Machinery, July 1989, Bradford, PRI, London, pp. 6/1–8
2 Day, A. J., Allport, J. M., Fischer, W. P., Coates, P. D. and Mimaroglu, A. Proceedings of ABAQUS User Conference, Aachen, June 1993, HKS Inc., Rhode Island, pp. 151–164
3 Cogswell, F. N. 'Polymer Melt Rheology', Godwin, Harlow, 1981
4 Tadmor, Z. and Gogos, C. G. 'Principles of Polymer Processing', Wiley, New York, 1979

5 Coates, P. D. and Ward, I. M. *J. Mater. Sci.* 1980, **15**, 2897
6 Coates, P. D. and Ward, I. M. *J. Mater. Sci.* 1978, **13**, 1957
7 G'Sell, C., Hiver, J. M., Dahoun, A. and Souahi, A. *J. Mater. Sci.* 1992, **27**, 5031
8 Sharpe, D. PhD Thesis, University of Bradford, 1986
9 Coates, P. D. and Sharp, D. A. Polymer Processing Society 3rd Annual Meeting, Stuttgart, April 1987
10 Ryan, J., Coates, P. D., Johnson, A. F., Hynds, J. and Patrick, P. *Plast. Rubber Process. Applic.* 1990, **13**(2), 121
11 Speight, R. G. and Coates, P. D. Proceedings of 4th International Conference on Polymer Processing Machinery, July 1991, London, PRI, London, pp. 15/1–12
12 Speight, R. G., Coates, P. D., Day, A. J. and Hull, J. B. Proceedings of Polymer Processing Society 9th annual conference, Manchester, April 1993
13 Speight, R. G. PhD Thesis, University of Bradford, 1993
14 Malloy, R. A., Chen, S. J., Orroth, S. A. and Farren, P. J. Proceedings of 3rd International Conference on Polymer Processing Machinery, July 1989, Bradford, PRI, London, pp. 9/1–12
15 Gibson, A. G. in 'Rheological Measurement' (Eds A. A. Collyer and D. W. Clegg), Elsevier, London, 1988
16 Rose, R. M., Coates, P. D. and Wilkinson, B. Proceedings of 3rd International Conference on Polymer Processing Machinery, July 1989, Bradford, PRI, London, pp. 13/1–9
17 Coates, P. D., Chohan, R. K., Groves, D. J., Speight, R. G., Rose, R. M. and Woodhead, M. Proceedings of Polymer Processing Society 9th annual conference, Manchester, April 1993
18 Coates, P. D., Ellis, D. I. and Pourmahnaei, S. M. *Plast. Rubber Process. Applic.* 1987, **8**, 165
19 Sweeney, J. and Ward, I. M. Proceedings of 13th Riso International Symposium on Materials Science: Modelling of Plastic Deformation and its Engineering Applications, Roskilde, Denmark, September 1992
20 Chohan, R. K., Coates, P. D. and Groves, D. J. Proceedings of Polymer Processing Society 9th annual conference, Manchester, April 1993